

Smooth transformations and ruling out closed orbits in planar systems

Tiemo Pedergnana and Nicolas Noiray

CAPS Laboratory, Department of Mechanical and Process Engineering, ETH Zürich, Sonneggstrasse 3, 8092 Zürich, Switzerland

(*Electronic mail: noirayn@ethz.ch)

(*Electronic mail: ptiemo@ethz.ch)

(Dated: November 28, 2023)

This work deals with planar dynamical systems with and without noise. In the first part, we seek to gain a refined understanding of such systems by studying their differential-geometric transformation properties under an arbitrary smooth mapping. Using elementary techniques, we obtain a unified picture of different classes of dynamical systems, some of which are classically viewed as distinct. We specifically give two examples of Hamiltonian systems with first integrals, which are simultaneously gradient systems. Potential applications of this apparent duality are discussed. The second part of this study is concerned with ruling out closed orbits in steady planar systems. We reformulate Bendixson's criterion using the coordinate-independent Helmholtz decomposition derived in the first part, and we derive another, similar criterion. Our results allow for automated ruling out of closed orbits in certain regions of phase space, and could be used in the future for efficient seeding of initial conditions in numerical algorithms to detect periodic solutions.

Planar dynamical systems can exhibit a broad range of complicated dynamics, some of which remain elusive even today. While great simplifications are available for Hamiltonian or gradient systems, the general Helmholtz decomposition has so far found little application in nonlinear dynamics. Since dynamical systems can be defined ad-hoc, for example, to model phase transitions or biological processes, the choice of basis for a given system may be ambiguous, which makes identification of the Helmholtz decomposition a nontrivial task. In contrast, mechanical systems generally have a known, preferred basis. In the first part of this work, we study bivariate Langevin equations under an arbitrary smooth mapping to obtain the transformation properties of their Helmholtz decomposition. This investigation reveals a unified picture of different classes of planar systems, some of which are typically presented as distinct. Specifically, we give two explicit examples of Hamiltonian systems with first integrals which are simultaneously gradient systems. In the second part, we discuss criteria for ruling out closed orbits in steady planar systems. We reformulate Bendixson's criterion in terms of the coordinate-independent Helmholtz decomposition derived in the first part, and we present another criterion for ruling out closed orbits. These latter results could help simplify numerical algorithms to detect periodic solutions in planar flows.

I. OVERVIEW

A. Dynamical system

In this work, we study planar (stochastic) dynamical systems given by a bivariate Langevin equation of the form¹⁻³

$$\dot{x} = \mathcal{F}(x, t) + \mathcal{B}(x)\Xi, \quad (1)$$

which is defined on a subset of the plane $\mathcal{D} \subset \mathbb{R}^2$.⁴ Equation (1) states that the evolution of the random variable $x: \mathbb{R}^+ \rightarrow \mathbb{R}^2$ over time $t \in \mathbb{R}^+$ is governed by the smooth velocity field $\mathcal{F}(x, t): \mathbb{R}^2 \times \mathbb{R}^+ \rightarrow \mathbb{R}^2$, the diffusion tensor $\mathcal{B}: \mathbb{R}^2 \times \mathbb{R}^+ \rightarrow \mathbb{R}^{2 \times 2}$ and the vector $\Xi = (\xi_1, \xi_2)^T$, whose entries are white Gaussian noise sources with variance Γ and zero mean.¹ Note that, if either $\Gamma = 0$ or \mathcal{B} vanishes identically for all $x \in \mathcal{D}$, the system given by Eq. (1) defines a deterministic planar flow with velocity field \mathcal{F} .^{5,6} (see pp. 42–65 and pp. 125–306, respectively) Unless explicitly stated otherwise, all quantities are assumed to be real in this work.

B. Helmholtz decomposition

Helmholtz's theorem^{7,8} states that, under certain conditions, a smooth, planar velocity field u can be decomposed as follows:⁹ (pp. 52–54)

$$u(x, t) = -\nabla\mathcal{V}(x, t) + S\nabla\mathcal{H}(x, t), \quad (2)$$

where $[\nabla(\cdot)]_m = \partial(\cdot)/\partial x_m$, \mathcal{V} is the scalar potential, \mathcal{H} is the Hamiltonian function and

$$S = \begin{pmatrix} 0 & 1 \\ -1 & 0 \end{pmatrix}. \quad (3)$$

The two-dimensional (2D) Helmholtz decomposition (HD) (2) can be derived from the three-dimensional case given in the above references by setting the vector potential equal to $(0, 0, \mathcal{H})^T$. We call \mathcal{H} the Hamiltonian function because for $\mathcal{V} = 0$, Eq. (2) corresponds to the definition of a canonical Hamiltonian velocity field.¹⁰ The restriction to the 2D case is motivated by the fact that for planar vector fields, the Helmholtz decomposition requires no special gauge conditions, since the number of potentials is equal to the number of entries of u . Nevertheless, there is some ambiguity in the decomposition (2): Adding a constant to

\mathcal{V} or \mathcal{H} does not change u defined in Eq. (2). Furthermore, a spatially constant term on the right-hand-side (RHS) of Eq. (1) can be included as a linear (monomial) term either in \mathcal{V} or in \mathcal{H} . See Appendix B for an example. No such ambiguity occurs in higher-order polynomial terms in a broad class of planar systems representing nonlinear oscillators, as shown in Appendix C. The HD is broadly used in fluid mechanics,^{11–18} electromagnetics,^{19–22} geophysics,^{23–25} imaging^{26,27} and computer vision.^{28–30} The reader interested in mathematical discussions of the HD,^{31–36} its generalization to n -dimensional vector fields³⁷ or a review of its applications³⁸ is referred to the respective literature. Uniqueness or existence are not of concern in this work, which is focused on the transformation properties of the HD (2) for smooth planar fields. Therefore, in the following, we generally assume that a (quasi)-unique decomposition exists throughout \mathcal{D} , such that Eq. (2) serves as a definition of u .

C. Transformation properties

In expressing the HD by Eq. (2), the use of Cartesian (rectangular) coordinates was tacitly assumed.⁹ (see pp. 21–52) With this in mind, we can study the dynamics of a planar dynamical system under additive white noise, $\dot{x} = u + \Xi$, in such coordinates. By Eq. (2), such a system can be written as

$$\dot{x} = -\nabla\mathcal{V}(x,t) + S\nabla\mathcal{H}(x,t) + \Xi. \quad (4)$$

At first sight, comparing Eqs. (1) and (4) is sensible only in the special case when \mathcal{B} corresponds to the 2-by-2 identity matrix. However, under an arbitrary, smooth mapping (see Fig. 1)

$$x = f(y), \quad (5)$$

after redefining $y \rightarrow x$, Eq. (4) is transformed into the following system:

$$\dot{x} = -g^{-1}(x)\nabla\tilde{\mathcal{V}}(x,t) \pm \frac{1}{\sqrt{\det[g(x)]}}S\nabla\tilde{\mathcal{H}}(x,t) + h(x)^{-1}\tilde{\Xi}, \quad (6)$$

where $J = \nabla f$ is the Jacobian matrix of the mapping f , $J = Qh$ is the polar decomposition of J ,³⁹ (see p. 449) $Q = Q^{-T} \in \mathbb{R}^{2 \times 2}$ is orthogonal, $h \in \mathbb{R}^{2 \times 2}$ is positive definite, $(\cdot)^T$ is the transpose, $g = h^T h \in \mathbb{R}^{2 \times 2}$ is the positive definite metric tensor of the mapping f , $\det(\cdot)$ is the determinant, $\tilde{\mathcal{V}}(x,t) = \mathcal{V}(f(x),t)$ is the transformed scalar potential and $\tilde{\mathcal{H}}(x,t) = \mathcal{H}(f(x),t)$ is the transformed Hamiltonian. The “ \pm ”-sign in Eq. (6) indicates whether Q is purely rotational ($\det Q = 1$, “+”) or if it contains a reflection ($\det Q = -1$, “-”). By the positive definiteness of h , $\det h(x) = \sqrt{\det g(x)}$ is positive.⁴⁰ We also mention the implicit assumption in the derivation of Eq. (6) that the transformed noise term $\tilde{\Xi}$ is related to its original counterpart by⁴¹ (see Sec. III. B.) $\Xi = Q(x)\tilde{\Xi}$. It is understood that the expression on the RHS of Eq. (6) is valid only in an open neighborhood in which g

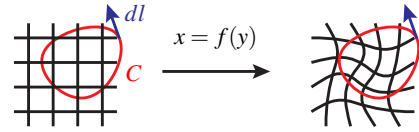


Figure 1. This work is concerned with smooth transformations and ruling out closed orbits in planar dynamical systems $\dot{x} = u(x,t)$. An example of a closed orbit is shown in red in the figure, superimposed on a transformed coordinate grid (black). Shown in blue is the tangent vector dl to the curve C at a certain point.

is non-singular. See pp. 172–182 of Guillemin and Pollack⁴² for a detailed discussion. The transformation formula defined by Eq. (6) is exemplified on the noise-driven, forced-damped Harmonic oscillator in Sec. B.

The first and last terms on the RHS of Eq. (6) have been derived for arbitrary-dimensional systems in previous work.⁴¹ The present study complements those results for the planar case by adding the transformed Hamiltonian term. If we drop all other terms and assume $\det Q = 1$, the transformed Hamiltonian system reads

$$\dot{x} = \frac{1}{\sqrt{\det[g(x)]}}S\nabla\tilde{\mathcal{H}}(x,t). \quad (7)$$

which is consistent with earlier works.^{43,44} If a given system can be identified to be of the form (7), there exist sets of preferred coordinates for that system, namely those in which $\det g$ becomes unity, leading to a canonical Hamiltonian system.

D. Steady planar flows

An important feature of steady planar flows

$$\dot{x} = u(x), \quad (8)$$

is the existence or absence of a closed orbit C in the phase space (see Fig. 1).⁴⁵ Determining the number of limit cycles in a given steady planar system is a nontrivial task⁴⁶ which can be tackled using numerical methods⁴⁷ or bifurcation theory^{5,48}. Determining an upper limit to the number of limit cycles in polynomial systems of the form (8) is also an open question and part of Hilbert’s 16th problem.^{49,50}

There exist few simple, analytical criteria to rule out closed orbits in steady planar systems.^{5,6} (see p. 44 and pp. 201–205, respectively) One example of such a criterion is Dulac’s criterion, which states that if there exists a smooth function $\varphi = \varphi(x)$ (the Dulac function⁵¹) such that the divergence of φu has only one sign throughout a simply connected domain \mathcal{D} , then Eq. (8) has no closed orbits⁵² which are entirely contained \mathcal{D} .⁶ (p. 204) In the special case where $\varphi = \text{const.}$, Dulac’s criterion reduces to Bendixson’s criterion.⁵ (see p. 44)

Combining the main result from the previous section, Eq. (6), with the theory of Jost⁵³, we show in Appendix A that Bendixson’s criterion can be reformulated as a statement which only concerns the scalar potential $\tilde{\mathcal{V}}$ of u :

Theorem 1 (Reformulation of Bendixson’s criterion) *If the scalar potential $\tilde{\mathcal{V}}$, or its negative $-\tilde{\mathcal{V}}$, of the planar field*

$$u(x) = -g^{-1}(x)\nabla\tilde{\mathcal{V}}(x) \pm \frac{1}{\sqrt{\det[g(x)]}}S\nabla\tilde{\mathcal{H}}(x), \quad (9)$$

is a strictly subharmonic function throughout a simply connected subset of the plane $\mathcal{D} \subset \mathbb{R}^2$, then the system $\dot{x} = u(x)$, $u = (u_1, u_2)^T$, has no closed orbits contained entirely in \mathcal{D} .

This result suggests that the Helmholtz decomposition is, to some degree, meaningful for (steady) planar systems, as the function $\tilde{\mathcal{V}}$ alone can rule out the existence of closed orbits, regardless of the form of $\tilde{\mathcal{H}}$.

In Sec. III B, we analytically derive another criterion for ruling out closed orbits. This criterion is first tested on classic examples of linear and nonlinear oscillators and then on the system of Shi Singlong,^{25,54} an example of a quadratic planar system with exactly four limit cycles.⁵⁵ We note that four is the maximal number of limit cycles in a quadratic planar system known to date.⁵⁰

II. RELATION TO PRIOR WORK

There exists a substantial literature on decompositions of smooth vector fields and on dynamical systems with Hamiltonian, gradient or mixed structure. This section seeks to connect the findings of the present work to those prior efforts. The derivation of the transformation formula in Eq. (6) partly overlaps with Sec. 3.4.2 of Risken³. The present work differs from Risken’s derivation in that, by writing out the Helmholtz decomposition explicitly, further simplifications are enabled. For example, the orthogonal matrix Q from the polar decomposition of the Jacobian essentially drops out of the transformed dynamics, which is not evident in the reference. In this regard, we also mention the Lamperti transform⁵⁶ (p. 98–100), which can be used to transform multiplicative to additive noise in one-dimensional stochastic systems.

The coordinate-independent formulation of the Helmholtz decomposition in Eq. (6) (set $\tilde{\Xi} = 0$ for comparison) is a special case of the Helmholtz–Hodge decomposition theorem⁵⁷ (p. 539), applied to planar systems. Other concepts related to this work are Poisson structures and Poisson brackets^{10,58} (pp. 381–387 and pp. 456–468). In the language of Olver⁵⁸, for example, the matrix $\sqrt{\det g}^{-1}S$ is the structure matrix for the Poisson bracket associated with the Hamiltonian system described by Eq. (7) in the steady case. Quispel and Capel⁵⁹ denote (steady) systems of the form of Eq. (7) simply as “Poisson systems”. McLachlan, Quispel, and Robidoux⁶⁰ show that any system with a first integral (a conserved quantity) can be written as a Poisson system (see McLachlan, Quispel, and Robidoux⁶¹ for the corresponding proofs). By combining these prior results with the present work, it becomes evident that, in the planar case, systems with first integrals are mapped into canonical, steady Hamiltonian systems by smooth transformations.

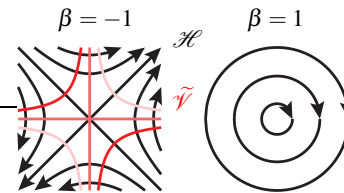


Figure 2. For $\beta > 0$, Eq. (10) describes the Harmonic oscillator. For $\beta < 0$, this system can simultaneously be described as governed by a Hamiltonian \mathcal{H} or as driven by the gradient of a scalar potential $\tilde{\mathcal{V}}$. Superimposing the isocontours of \mathcal{H} (black) and $\tilde{\mathcal{V}}$ (red, more saturated colors correspond to larger values) for $\beta = -1$ reveals an intuitive picture: the potential landscape drives trajectories along the isocontours of the Hamiltonian. Arrows indicate the direction of the flow.

McLachlan, Quispel, and Robidoux⁶⁰ further show that any system with a strict (strictly decreasing along trajectories) Lyapunov function can be written as $\dot{x} = -g^{-1}(x)\nabla\tilde{\mathcal{V}}$, where g is a positive definite matrix. Such systems have been shown to derive from gradient-driven dynamics, subjected to an arbitrary smooth mapping f .⁴¹ The combination of the above results implies that smooth transformations map systems with strict Lyapunov functions into canonical gradient systems, which is also consistent with the work of Bárta, Chill, and Fařangová⁶².

In standard textbooks on nonlinear dynamics, gradient systems and Hamiltonian systems are presented separately.^{5,6} However, assuming these classes of systems to be inherently distinct would be a false dichotomy. In general, a given system can *simultaneously* be a gradient system and a Hamiltonian system, which is already evident in the trivial system $\dot{x} = 0$. For an explicit, nontrivial example, consider the canonical Hamiltonian system

$$\dot{x} = \begin{pmatrix} 0 & 1 \\ -1 & 0 \end{pmatrix} \nabla\mathcal{H}(x), \quad (10)$$

$x = (x_1, x_2)^T$, with $\mathcal{H}(x) = \beta x_1^2/2 + x_2^2/2$. If $\beta > 0$, this system corresponds to the Harmonic oscillator. However, for *any* β , this system is Hamiltonian and has a first integral: $d\mathcal{H}/dt = 0$. Now, note that the same system can be rewritten as

$$\dot{x} = - \underbrace{\begin{pmatrix} 1 & 0 \\ 0 & -\beta \end{pmatrix}}_{=g^{-1}(x)} \nabla\tilde{\mathcal{V}}(x), \quad (11)$$

where $\tilde{\mathcal{V}} = -x_1x_2$. For $\beta < 0$, the matrix $g^{-1} = \text{diag}(1, -\beta)$ is positive definite, i.e., Eq. (11) represents a (transformed) gradient system.⁴¹ Note that, in this parameter range, the isocontours of \mathcal{H} describe hyperbolas in the plane, as shown in Fig. 2. For $\beta = -1$, g becomes equal to the identity matrix, and the contours of $\tilde{\mathcal{V}}$ are exactly orthogonal to those of \mathcal{H} : the potential landscape drives the system’s trajectories along the energy levels of the Hamiltonian. The same is not true for $\beta \neq -1$, as g skews the gradient dynamics, leading the trajectories to not follow exactly the steepest descent. For $\beta < 0$, the

real mapping $f(x) = (x_1, x_2 \sqrt{-\beta})^T$, for instance, transforms Eq. (11) back into a canonical gradient system $\dot{x} = -\nabla \mathcal{V}$, and Eq. (10) into $\dot{x} = \sqrt{\det g}^{-1} S \nabla \widetilde{\mathcal{H}}$. In these preferred coordinates, the isocontours of \mathcal{V} are always perpendicular to those of $\widetilde{\mathcal{H}}$. Another example of a system which is simultaneously a gradient system and a Hamiltonian system is given in Sec. IV B.

III. MAIN RESULTS

A. Transformed Hamiltonian systems

Since the gradient and noise terms in Eq. (6) have already been derived,⁴¹ what is left is to obtain the transformation formula for the Hamiltonian system $\dot{x} = S \nabla \widetilde{\mathcal{H}}$ under a general mapping of the form (5). For this, we set $x = f(y)$ and apply the chain rule to this system in index form:

$$\dot{x}_m = S_{mn} \frac{\partial \widetilde{\mathcal{H}}(f(y), t)}{\partial x_n}, \quad (12)$$

$$\frac{\partial x_m}{\partial y_k} \dot{y}_k = S_{mn} \frac{\partial y_l}{\partial x_n} \frac{\partial \widetilde{\mathcal{H}}(y, t)}{\partial y_l}, \quad (13)$$

$$\dot{y}_k = \underbrace{\frac{\partial y_k}{\partial x_m} S_{mn}}_{\widetilde{S}_{kl}} \frac{\partial y_l}{\partial x_n} \frac{\partial \widetilde{\mathcal{H}}(y, t)}{\partial y_l}, \quad (14)$$

where the time-dependence of x and y was suppressed for brevity. In Eq. (14), we defined the matrix \widetilde{S} , whose entries are given by

$$\widetilde{S}_{kl} = \frac{\partial y_k}{\partial x_m} S_{mn} \frac{\partial y_l}{\partial x_n} \quad (15)$$

$$= \frac{\partial y_k}{\partial x_1} \frac{\partial y_l}{\partial x_2} - \frac{\partial y_k}{\partial x_2} \frac{\partial y_l}{\partial x_1} \quad (16)$$

$$\implies \widetilde{S} = \left(\frac{\partial y_1}{\partial x_1} \frac{\partial y_2}{\partial x_2} - \frac{\partial y_1}{\partial x_2} \frac{\partial y_2}{\partial x_1} \right) S. \quad (17)$$

To interpret this result, we note that the term in brackets is simply the determinant of the Jacobian of the inverse mapping $y = f^{-1}(x)$. By the properties of the determinant,³⁹ (see pp. 8–12) we conclude that

$$\frac{\partial y_1}{\partial x_1} \frac{\partial y_2}{\partial x_2} - \frac{\partial y_1}{\partial x_2} \frac{\partial y_2}{\partial x_1} = [\det J(y)]^{-1}. \quad (18)$$

A further simplification is enabled by the polar decomposition $J = Qh$, where Q is an orthogonal matrix with $\det(Q) = \pm 1$. Note that $\det J = \det Q \det h$ and $\det h = \sqrt{\det g}$. Collecting the above results, we have shown that under a general mapping f , a planar Hamiltonian system transforms like

$$S \nabla \widetilde{\mathcal{H}}(x, t) \rightarrow \pm \frac{1}{\sqrt{\det[g(y)]}} S \nabla_y \widetilde{\mathcal{H}}(y, t), \quad (19)$$

where $(\nabla_y)_m = \partial/\partial y_m$ and the transformed Hamiltonian is defined as $\widetilde{\mathcal{H}}(y, t) = \mathcal{H}(f(y), t)$. Redefining $y \rightarrow x$, $\nabla_y \rightarrow \nabla$ in Eq. (19) and combining this formula with previous results⁴¹ yields Eq. (7).

B. Ruling out closed orbits

Dulac's criterion concerns the autonomous planar dynamical system defined by Eq. (8), which is governed by the smooth vector field u defined on a simply connected domain $\mathcal{D} \subset \mathbb{R}^2$. The criterion states that if there exists a smooth function $\varphi = \varphi(x)$ (the Dulac function⁵¹) such that the divergence of φu has only one sign throughout \mathcal{D} , then Eq. (8) has no closed orbits which are entirely contained in that region.⁶ (p. 204) Here, under the same assumptions on u and \mathcal{D} , we prove the following statement:

Theorem 2 *If there exists a smooth, positive definite 2-by-2 matrix function $\mathcal{N} = \mathcal{N}(x)$ with entries $\mathcal{N}_{mn}(x)$, $m, n \in \{1, 2\}$, such that the out-of-plane component ω of*

$$\text{curl} U(x) = \begin{pmatrix} 0 \\ 0 \\ \omega(x) \end{pmatrix}, \quad (20)$$

where

$$U(x) = \begin{pmatrix} \mathcal{N}_{11}(x)u_1(x) + \mathcal{N}_{12}(x)u_2(x) \\ \mathcal{N}_{21}(x)u_1(x) + \mathcal{N}_{22}(x)u_2(x) \\ 0 \end{pmatrix}, \quad (21)$$

is zero throughout a simply connected subset of the plane $\mathcal{D} \subset \mathbb{R}^2$, then the planar system $\dot{x} = u(x)$, $u = (u_1, u_2)^T$, has no closed orbits contained entirely in \mathcal{D} .

To prove Theorem 2, we assume that the out-of-plane-component of $\text{curl} U$, where U is defined in Eq. (21), is zero in \mathcal{D} . Integrating this expression over a simply connected subset \mathcal{R} of the domain \mathcal{D} bounded by the closed, positively oriented curve $C = \partial \mathcal{R}$, and applying Stokes' theorem⁹ (p. 43) yields

$$0 = \int_{\mathcal{R}} \omega(x) dA \quad (22)$$

$$= \int_{\mathcal{R}} [\text{curl} U(x)]^T n dA \quad (23)$$

$$= \oint_C u^T(x) \mathcal{N}^T(x) dl, \quad (24)$$

where dA is an infinitesimal area element, $n = (0, 0, 1)^T$ is the normal vector and dl is an infinitesimal tangent vector to C (compare Fig. 1). Along trajectories $x(t)$ governed by Eq. (8), $dl = u dt$.⁶ (p. 204) Therefore, if C is an orbit of the system given by Eq. (8), then it can be parametrized such that the RHS of Eq. (24) takes the following form:

$$\oint_C u^T(x(t)) \mathcal{N}^T(x(t)) u(x(t)) dt. \quad (25)$$

By the positive definiteness of \mathcal{N} (\Leftrightarrow of \mathcal{N}^T) and because C is chosen arbitrarily, the integral (25) generally has a positive sign,⁶³ in contradiction to the assumption that ω vanishes in \mathcal{D} . This contradiction shows that, under the assumptions of Theorem 2, \mathcal{D} can contain no closed curve Γ which is an orbit of the system governed by Eq. (8).

Theorem 2 can be applied in automated fashion by making, for example, a positive definite ansatz of the form

$$\mathcal{N}(x) = \begin{pmatrix} a(x_1) & \mathcal{N}_{12}(x_1, x_2) \\ 0 & b \end{pmatrix}, \quad (26)$$

or

$$\mathcal{N}(x) = \begin{pmatrix} c & 0 \\ \mathcal{N}_{21}(x_1, x_2) & d(x_2) \end{pmatrix}, \quad (27)$$

where a and d are arbitrary, positive functions of x_1 and x_2 , respectively, and $b, c \in \mathbb{R}^+$ are positive real numbers. We comment on this ansatz in Sec. V. Note that a, b, c and d can be arbitrarily specified, and are only restricted by their positivity. In the examples we consider below, substituting Eqs. (26) and (27) into U defined in Eq. (21) and requiring that $\text{curl} U = 0$ yields two linear first-order differential equations for each system, one in x_2 (for \mathcal{N}_{12}) and one in x_1 (for \mathcal{N}_{21}). In each of these equations, the other respective coordinate is treated as a parameter. If the solution of either of the resulting equations exists over a simply connected planar domain \mathcal{D} , then, by Theorem 2, there exists no closed orbit fully contained in \mathcal{D} . We note that, in a Cartesian basis, $\text{curl}(\cdot) = \nabla \times (\cdot)$ and $\omega = \partial U_1 / \partial x_2 - \partial U_2 / \partial x_1$, so that the differential equations resulting from Eqs. (26) and (27) are

$$-a(x_1) \frac{\partial u_1(x_1, x_2)}{\partial x_2} - \frac{\partial \mathcal{N}_{12}(x_1, x_2)}{\partial x_2} u_2(x_1, x_2) - \mathcal{N}_{12}(x_1, x_2) \frac{\partial u_2(x_1, x_2)}{\partial x_2} + b \frac{\partial u_2(x_1, x_2)}{\partial x_1} = 0, \quad (28)$$

$$-c \frac{\partial u_1(x_1, x_2)}{\partial x_2} + \frac{\partial \mathcal{N}_{21}(x_1, x_2)}{\partial x_1} u_1(x_1, x_2) + \mathcal{N}_{21}(x_1, x_2) \frac{\partial u_1(x_1, x_2)}{\partial x_1} + d(x_2) \frac{\partial u_2(x_1, x_2)}{\partial x_1} = 0, \quad (29)$$

respectively. The above results are summarized in the following corollary to Theorem 2:

Corollary 1 *If the steady planar system $\dot{x} = u(x)$ is formulated in Cartesian coordinates, it has no closed orbits contained entirely in any simply connected region in which a solution of either Eq. (28) or Eq. (29) exists.*

Let us now apply the mathematical tools presented in this section to specific examples.

IV. EXAMPLES

A. Kermack–McKendrick theory

A simplified version of Kermack and McKendrick’s mathematical theory of epidemics⁶⁴ is described by the following planar system with $x = (x_1, x_2)$ ⁶ (p. 188):

$$\dot{x} = \begin{pmatrix} -kx_1x_2 \\ kx_1x_2 - lx_2 \end{pmatrix}. \quad (30)$$

where $x_1 \geq 0$ denotes the healthy population, $x_2 \geq 0$ is the sick population and $k, l > 0$ are constants. While we note that the Hamiltonian structure of a similar, three-dimensional model has previously been analyzed,^{65,66} we focus here on the planar version. In the positive quadrant $x_1, x_2 > 0$, by comparison with Eq. (7), Eq. (30) represents a transformed Hamiltonian system of the form of Eq. (7) with

$$\sqrt{\det g(x)}^{-1} = kx_1x_2, \quad (31)$$

$$\widetilde{\mathcal{H}}(x) = \frac{l}{k} \ln x_1 - x_1 - x_2. \quad (32)$$

By Eq. (31), the determinant of the metric tensor is singular on the two axes. As a consequence, the system given by Eq. (30) can not be expressed in terms of the same transformed Hamiltonian $\widetilde{\mathcal{H}}$ throughout \mathbb{R}^2 .

B. Coupled Kuramoto oscillators

O’Keeffe, Ceron, and Petersen⁶⁷ derive, from two coupled Kuramoto oscillators, the following system, with $x = (y, \theta)$:

$$\dot{x} = \begin{pmatrix} -\mathcal{J} \sin y \cos \theta, \\ -\mathcal{K} \sin \theta \cos y, \end{pmatrix} \quad (33)$$

where \mathcal{J} and \mathcal{K} are coupling constants (see pp. 7–8 of the reference). We showed in our previous work⁴¹ that this steady, planar system can be written as a transformed gradient system $\dot{x} = -g^{-1} \nabla \widetilde{\mathcal{V}}$ for $\mathcal{J}, \mathcal{K} > 0$. If, however, \mathcal{K} is less than zero, the same system has nested, closed orbits and there exists a conserved Hamiltonian $\widetilde{\mathcal{H}}(x)$.⁶⁷ In the positive quadrant $y, \theta > 0$, Eq. (33) is equivalent to a transformed Hamiltonian system of the form of Eq. (7) with⁶⁷ (see p. 7 for the derivation of $\widetilde{\mathcal{H}}$)

$$\sqrt{\det g(x)}^{-1} = \frac{(\sin y)^{\mathcal{K}+1}}{(\sin \theta)^{\mathcal{J}-1}}, \quad (34)$$

$$\widetilde{\mathcal{H}}(x) = -\frac{(\sin \theta)^{\mathcal{J}}}{(\sin y)^{\mathcal{K}}}. \quad (35)$$

Similar expressions can be found in each of the other quadrants from the requirement that $\det g$ is always positive. A nonsmooth Hamiltonian which describes the dynamics governed by Eq. (33) in each of the quadrants (but not along the axes) is given by $-|\widetilde{\mathcal{H}}|$, where $\widetilde{\mathcal{H}}$ is defined in Eq. (35). This quantity is visualized in Fig. 3 for different values of \mathcal{J} and \mathcal{K} . Note that the color map is cut off in the top row of Fig. 3. This is because the main emphasis of this figure is the *shape* of the isocontours, not their level values.

The Hamiltonian formulation of Eq. (33) given in Eqs. (34) and (35) is also true for $\mathcal{K} > 0$, where the system is known to be governed by the gradient of a steady potential $\widetilde{\mathcal{V}} = -\cos(y) \cos(\theta)$ and the metric tensor $g = \text{diag}(\mathcal{J}, \mathcal{K})$.⁴¹ In other words, for $\mathcal{K} > 0$, the system defined by Eq. (33) is simultaneously a Hamiltonian system and a gradient system. Consequently, in this parameter range, $\widetilde{\mathcal{H}}$ can have no closed

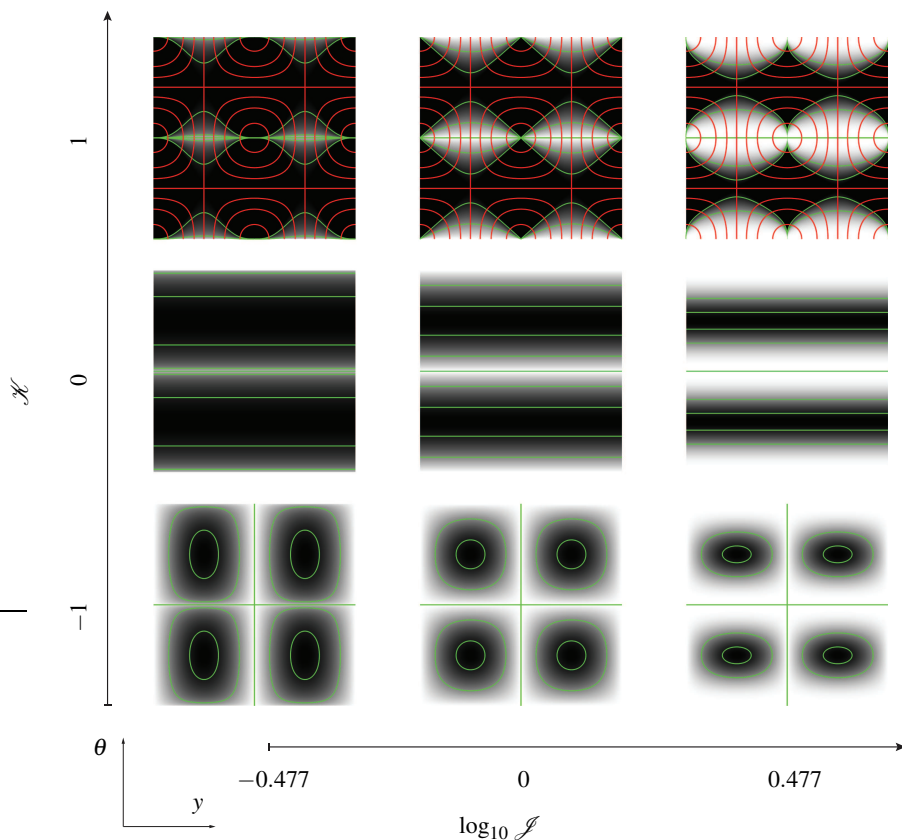


Figure 3. Illustration of the Hamiltonian governing a system of coupled Kuramoto oscillators discussed in Sec. IV B, over the coupling constants \mathcal{J} and \mathcal{K} (semi-log scale). Shown are contour plots of $-\|\tilde{\mathcal{H}}\|$, where $\tilde{\mathcal{H}}$ is defined by Eq. (35), over the periodic domain $[-\pi, \pi] \times [-\pi, \pi]$, ranging from values of -1 (black) to 0 (white), overlaid with selected contour lines (green). In the cases with $\mathcal{K} = 1$, the colormap was cut off at ± 1 because $\tilde{\mathcal{H}}$ shows singular behavior. In the top row of this figure, the isocontours of the scalar potential $\tilde{\mathcal{V}} = -\cos(y)\cos(\theta)$ derived in prior work,⁴¹ governing the same system for $\mathcal{J}, \mathcal{K} > 0$, are overlaid in red over the isocontours of $\tilde{\mathcal{H}}$.

isocontours, because this property would be in contradiction to its gradient-driven nature for positive \mathcal{J} and \mathcal{K} .⁶ (pp. 201–202) This argument is confirmed by the visualization of the Hamiltonian $\tilde{\mathcal{H}}$ in Fig. 2. This figure shows that, as expected, when \mathcal{K} is varied from negative to positive values, the contours of $\tilde{\mathcal{H}}$ lose their closed character. In the top row of Fig. 3, the isocontours of the scalar potential $\tilde{\mathcal{V}}$ are overlaid in red over the isocontours of $\tilde{\mathcal{H}}$. Similar to the example in Sec. (II), for $\mathcal{J} = \mathcal{K} = 1$ (top row, middle inset of Fig. 3), g equals the identity matrix and the isocontours of $\tilde{\mathcal{V}}$ are perpendicular to those of $\tilde{\mathcal{H}}$.

C. Strogatz's conservative system

Strogatz proposes the following conservative system with $x = (x_1, x_2)$:⁶ (p. 190)

$$\dot{x} = \begin{pmatrix} x_1 x_2 \\ -x_1^2 \end{pmatrix}. \quad (36)$$

By comparison with Eq. (7), in the right half-plane $x_1 > 0$, this system is a transformed Hamiltonian system with

$$\sqrt{\det g(x)}^{-1} = x_1, \quad (37)$$

$$\tilde{\mathcal{H}}(x) = \frac{x_1^2 + x_2^2}{2}. \quad (38)$$

A similar expression can be found for the left half-plane.

D. Limit cycle scattering

We consider a stochastic extension of the model introduced in Pedergnana and Noiray⁶⁸ to model superradiant scattering by a limit cycle:

$$\dot{a} = \left(i\omega_0 - \gamma a + \frac{\beta}{1 + \kappa|a|^2} \right) + D s e^{i\omega t} + Z, \quad (39)$$

where a is the complex modal amplitude, i is the imaginary unit, ω_0 is the eigenfrequency, γ is the damping, β is the linear gain, κ is the saturation constant, D_j is the j^{th} entry of the coupling matrix D , s is the incident wave amplitude, ω is the

frequency of the incident wave, $Z = \xi_1 + i\xi_2$, and $\xi_{1,2}$ are white Gaussian noise sources. Defining $A = |a|$, $\phi = \arg(a)$, $\varphi = \phi - \omega t$ and separating real and imaginary parts yields, with $x = (A, \varphi)^T$,

$$\dot{A} = -\gamma A + \frac{\beta A}{1 + \kappa A^2} + |D_j|s \cos(\arg D_j + \varphi) + \xi_1, \quad (40)$$

$$\dot{\varphi} = \Delta - \frac{|D_j|s \sin(\arg D_j + \varphi)}{A} + \frac{\xi_2}{A}, \quad (41)$$

where $\Delta = \omega_0 - \omega$ is the detuning. In the absence of an incident wave ($s = 0$), Eqs. (40) and (41) describe a stable limit cycle $a_0(t) = A_0 e^{i\omega_0 t}$ with constant amplitude $A_0 = \sqrt{(\beta/\gamma - 1)/\kappa}$. Assuming a curvilinear basis with $g = \text{diag}(1, A^2)$ and $\sqrt{\det g} = A$ (see also Appendix B), a transformed Helmholtz decomposition in the form of Eq. (6) of the system given by Eq. (39) is readily found to be

$$\tilde{\mathcal{V}}(x) = \frac{\gamma A^2}{2} - \frac{\beta \log(\kappa A^2 + 1)}{2\kappa} - |D_j|sA \cos(\varphi + \arg(D_j)), \quad (42)$$

$$\tilde{\mathcal{H}}(x) = \frac{\Delta A^2}{2}, \quad (43)$$

with the inverse metric tensor $g^{-1} = \text{diag}(1, A^{-2})$ and the positive definite matrix $h^{-1} = \text{diag}(1, A^{-1})$ multiplying the noise vector Ξ . Unless ω is set to ω_0 (no detuning), which makes the system given by Eq. (39) purely driven by the steady scalar potential, the interplay between the Hamiltonian and gradient parts of the Helmholtz decomposition is not easy to grasp. In contrast, the following alternative formulation with pure, but time-dependent, gradient is straightforward to interpret. This alternative description is obtained by absorbing the detuning Δ into the shifted phase $\Phi = \varphi - \Delta t$, leading to:

$$\tilde{\mathcal{V}}(x, t) = \frac{\gamma A^2}{2} - \frac{\beta \log(\kappa A^2 + 1)}{2\kappa} - |D_j|sA \cos(\Phi + \Delta t + \arg(D_j)), \quad (44)$$

$$\tilde{\mathcal{H}}(x) = 0, \quad (45)$$

with $x = (A, \Phi)^T$ and $g = h^T h = \text{diag}(1, A^{-2})$. Equations (44) and (45) also describe a Helmholtz decomposition (6) of the system defined by Eq. (39). As discussed in prior work on a similar example,⁴¹ (Sec. V. A.) the explicit and periodic time-dependence of the potential $\tilde{\mathcal{V}}$ in Eq. (44) corresponds to beating oscillations of A and φ (see Fig. (4)). For small detuning $\Delta \ll \omega$, these oscillations are slow compared to the forcing by the incident wave, and the system can be approximated as perfectly synchronized to good accuracy. The unsteady potential formulation given in Eqs. (44) and (45) reveals explicitly the time-dependent, deterministic forcing of the amplitude-phase dynamics for nonzero detuning, which is not directly evident from the steady, mixed Helmholtz decomposition given by Eqs. (42) and (43). Potential future applications of the unsteady potential formulation are discussed in Sec. V.

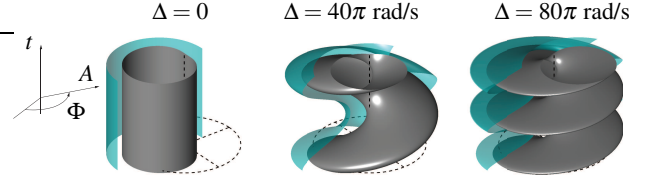


Figure 4. Isosurfaces of the unsteady potential (44) governing super-radiant scattering by a limit cycle.⁶⁸ The parameter values used to generate this figure correspond to those used in Fig. 3(a) in the reference. The variable parameter $\Delta = \omega_0 - \omega$ denotes the detuning between the incident wave and the eigenfrequency of the limit cycle. The radius of the dashed circle corresponds to $10A_0$, where A_0 is the unforced limit cycle amplitude. The dashed vertical line's length is $(\beta - \gamma)^{-1}$. The gray and cyan surfaces correspond to 0.5% and 5% of the maximum value of $\tilde{\mathcal{V}}$ over the domain $[-20A_0, 20A_0] \times [-20A_0, 20A_0] \times [0, (\beta - \gamma)^{-1}]$. The explicit time-dependence visible in this figure arises from the interplay between the Hamiltonian and gradient parts of the Helmholtz decomposition in a steady system.

We note that no term proportional to A^{-1} appears in the modal dynamics defined by Eq. (39), which would be the case had these equations been consistently derived by deterministic⁶⁹ and stochastic averaging^{1,70} of a corresponding “fast oscillating” system (see, for instance, Noiry⁷¹). Such a fast system may involve more intricate synchronization dynamics.⁷² Exploring the equivalence class of systems leading to Eq. (39) via the averaging method, also in view of their Helmholtz decomposition (6), is a topic for future research.

E. Harmonic oscillator

To apply Theorem 2 and Corollary 1, we now consider the harmonic oscillator with $\omega_0 = 1$ in the undamped ($\gamma = 0$), unforced ($F = 0$), noise-free ($\Xi = 0$) limit, which is a steady planar Hamiltonian system $\dot{x} = S\nabla\mathcal{H}$ with $\mathcal{H}(x) = (x_1^2 + x_2^2)/2$ that possesses nested closed orbits in the form of circles (or ellipses, if the coordinates are not normalized) around the origin (see Fig. 3, left inset). In a Cartesian basis with normalized variables $x = (x_1, x_2)$ (see Sec. B), the dynamics read

$$\dot{x} = \underbrace{\begin{pmatrix} x_2 \\ -x_1 \end{pmatrix}}_{=u(x)}. \quad (46)$$

Substituting the velocity field $u(x)$ given by the RHS of Eq. (46) into Eqs. (28) and (29) yields the following set of differential equations:

$$-a(x_1) + \frac{\partial \mathcal{N}_{12}(x_1, x_2)}{\partial x_2} x_1 - b = 0, \quad (47)$$

$$-c + \frac{\partial \mathcal{N}_{21}(x_1, x_2)}{\partial x_1} x_2 - d(x_2) = 0. \quad (48)$$

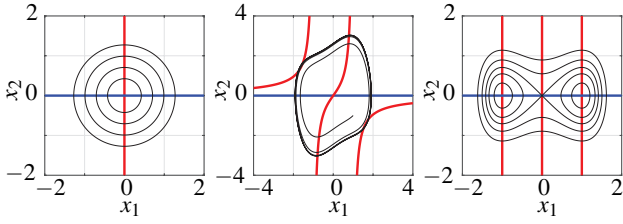


Figure 5. Illustration of the results derived in Sec. IV E, Sec. IV F, and Sec. IV G for the Harmonic (left), Van der Pol (middle) and Duffing oscillators (right), respectively. By Theorem 2, no closed orbits can be fully contained in any simply connected region throughout which a positive definite matrix function \mathcal{N} exists such that Eq. (22) is identically satisfied in that domain. Using Corollary 1, in Cartesian coordinates, two matrix functions satisfying this condition can be found by solving the first-order differential equations (28) and (29) for their respective off-diagonal elements. These solutions do *not* exist, but are singular, over the blue and red curves, respectively, shown in the figure. Therefore, any closed orbits of the systems (46), (51) and (56) must cross at least one blue and one red curve. Typical trajectories of all three systems are shown in black, demonstrating that Theorem 2 is indeed satisfied for these examples. In the middle inset, $\alpha = 0.7$.

The general solutions of Eqs. (47) and (48) are given by

$$\mathcal{N}_{12}(x_1, x_2) = \frac{[a(x_1) + b]x_2}{x_1} + C_1, \quad (49)$$

$$\mathcal{N}_{21}(x_1, x_2) = \frac{[c + d(x_2)]x_1}{x_2} + C_2, \quad (50)$$

where C_1 and C_2 are constants of integration. The expression (49) exists for $x_1 \neq 0$ (left and right half-plane) and (50) for $x_2 \neq 0$ (bottom and upper half-plane). None of these regions fully contain any closed orbits of the system defined by Eq. (46), confirming Theorem 2 and its Corollary 1. The above results are visualized, together with typical trajectories of Eq. (46), in Fig. 5 (left inset).

F. Van der Pol oscillator

Nearly a century ago, Balthasar Van der Pol proposed his nonlinear oscillator to describe self-sustained relaxation oscillations in electronic circuits.⁷³ To test Theorem 2, we consider here the following nondimensionalized set of equations describing an unforced Van der Pol oscillator⁵ (pp. 67–68):

$$\dot{x} = \begin{pmatrix} x_2 \\ -x_1 + \alpha(1 - x_1^2)x_2 \end{pmatrix} \quad (51)$$

where $\alpha \geq 0$ is a non-negative constant. Assuming a Cartesian basis and substituting the velocity field $u(x)$ given by the RHS of (51) into Eqs. (28) and (29) yields the following equations:

$$-a(x_1) - \frac{\partial \mathcal{N}_{12}(x_1, x_2)}{\partial x_2} (-x_1 + \alpha(1 - x_1^2)x_2) - \mathcal{N}_{12}(x_1, x_2)\alpha(1 - x_1^2) - b(1 + 2\alpha x_1 x_2) = 0, \quad (52)$$

$$-c + \frac{\partial \mathcal{N}_{21}(x_1, x_2)}{\partial x_1} x_2 - d(x_2)(1 + 2\alpha x_1 x_2) = 0. \quad (53)$$

These equations have the following general solutions:

$$\mathcal{N}_{12}(x_1, x_2) = \frac{[a(x_1) + b]x_2 + \alpha b x_1 x_2^2 + C_1}{x_1 - \alpha(1 - x_1^2)x_2}, \quad (54)$$

$$\mathcal{N}_{21}(x_1, x_2) = \frac{[c + d(x_2)]x_1}{x_2} + d(x_2)\alpha x_1^2 + C_2. \quad (55)$$

For $\alpha > 0$, the zero level set of the denominator of (54) describes a curve which crosses the origin and diverges to negative infinity at $x_1 = -1$ and to positive infinity at $x_1 = 1$. In general, \mathcal{N}_{12} exists everywhere but on this curve. Similarly, the solution (55) exists in the upper and in the lower half-plane, but not on the x -axis ($x_2 = 0$). The limit cycle of the Van der Pol oscillator,⁵ (pp. 67–82) which winds around the origin, necessarily crosses both of these curves, on which the solutions (54) and (55) do not exist, confirming Theorem 2. See Fig. 5, middle inset, for an illustration of the above results on an example with $\alpha = 0.7$.

G. Duffing nonlinearity

For our next example, we examine the Duffing oscillator⁷⁴ with a double-well Hamiltonian in nondimensionalized form⁵ (pp. 82–91):

$$\dot{x} = \begin{pmatrix} x_2 \\ x_1 - x_1^3 \end{pmatrix} \quad (56)$$

Equation (56) is of the form $\dot{x} = S\nabla \mathcal{H}$ with $\mathcal{H}(x) = (x_2^2 - x_1^2)/2 + x_1^4/4$ and is governed by two families of closed orbits, segregated by the curve $\mathcal{H}(x) = 0$, the separatrix. For $\mathcal{H} > 0$, the flow (56) has closed orbits encircling the separatrix and the fixed point at the origin. In the region where $\mathcal{H} < 0$, inside the separatrix, there are two nested sets of closed orbits, mirror-symmetric with respect to the y -axis, which wind around the fixed points $x = (-1, 0)^T$ and $x = (1, 0)^T$, respectively (see Fig. 5, right inset). Using a Cartesian basis, substituting the RHS of (56) into Eqs. (28) and (29) leads to

$$-a(x_1) - \frac{\partial \mathcal{N}_{12}(x_1, x_2)}{\partial x_2} (x_1 - x_1^3) + b(1 - 3x_1^2) = 0, \quad (57)$$

$$-c + \frac{\partial \mathcal{N}_{21}(x_1, x_2)}{\partial x_1} x_2 + d(x_2)(1 - 3x_1^2) = 0, \quad (58)$$

whose general solutions are given by

$$\mathcal{N}_{12}(x_1, x_2) = \frac{[b - a(x_1)]x_2 - 3bx_1^2 x_2}{x_1 - x_1^3} + C_1, \quad (59)$$

$$\mathcal{N}_{21}(x_1, x_2) = \frac{cx_1 + d(x_2)(x_1^3 - x_1)}{x_2} + C_2. \quad (60)$$

By Corollary 1, looking at Eqs. (59) and (60), any closed orbits of the steady planar system defined by Eq. (56) must cross one of the lines $x_1 = 1$, -1 or $x_1 = 0$ and, additionally, cross the x -axis $x_2 = 0$. By the above discussion, as shown in Fig. 5, right inset, these conditions are indeed satisfied, confirming Theorem 2.

H. Quadratic system with four limit cycles

We consider the system of Shi Songling^{54,75}, given by⁵⁵

$$\dot{x} = \begin{pmatrix} \lambda x_1 - x_2 - 10x_1^2 + (5 + \delta)x_1x_2 + x_2^2 \\ x_1 + x_1^2 + (-25 + 8\varepsilon - 9\delta)x_1x_2 \end{pmatrix}, \quad (61)$$

for the parameter values $\delta = -10^{-13}$, $\varepsilon = -10^{-52}$ and $\lambda = -10^{-200}$. This system has exactly four limit cycles. Three of the limit cycles are tiny (see Fig. 2 of Galias and Tucker⁵⁵) and encircle the point $(0,0)$, while the fourth is normalized and encircles $(0,1)$. The interested reader is referred to Kuznetsov, Kuznetsova, and Leonov⁷⁶ for a quadratic planar system with four normal-sized limit cycles. The solutions of Eqs. (28) and (29) for the system given by Eq. (61) are of the form

$$\mathcal{N}_{12}(x_1, x_2) = \frac{X(x_1, x_2) + C_1}{x_1 + x_1^2 + (-25 + 8\varepsilon - 9\delta)x_1x_2}, \quad (62)$$

$$\mathcal{N}_{21}(x_1, x_2) = \frac{Y(x_1, x_2) + C_2}{\lambda x_1 - x_2 - 10x_1^2 + (5 + \delta)x_1x_2 + x_2^2}, \quad (63)$$

where, for suitable choices of $a(x_1)$ and $d(x_2)$, X and Y are compositions of smooth, elementary functions. The curves on which \mathcal{N}_{12} and \mathcal{N}_{21} are singular are visualized in Fig. 6. These curves intersect at the points $(0,0)$ and $(0,1)$. We observe that the distance between the intersection at the origin and a nearby critical point is small. In a (semi-)automated analysis, this distance could be used as a first estimate of the length scale at which the dynamics near the origin take place, determining the discretization fineness of initial conditions seeded along the singularity curves of \mathcal{N}_{12} and \mathcal{N}_{21} .

V. DISCUSSION AND OUTLOOK

This work explores smooth transformations of planar systems. It was shown in Sec. II and in Sec. IV B that Hamiltonian systems without closed isocontours can simultaneously be gradient systems. In light of these results, it would be worth investigating if one could consistently define a gradient system from such a Hamiltonian and vice versa. If so, then this dualism may help towards quantization⁷⁷ of systems which are not purely Hamiltonian, which is a topic of ongoing research with theoretical and practical significance.^{78–81} A geometric approach to unifying Hamiltonian and gradient dynamics is taken by Esen, Grmela, and Pavelka⁸². To analyze the saddle-type Hamiltonians discussed here, it may prove useful to introduce hyperbolic action-angle coordinates in the spirit of Waalkens, Schubert, and Wiggins⁸³ (see pp. 25–26).

In Sec. IV D, an example was given of a steady planar system with nonzero Hamiltonian and gradient part. It was shown that this system can alternatively be written as an *unsteady*, purely gradient-driven system with vanishing Hamiltonian part, complementing earlier results.⁴¹ It could be interesting to study whether such a reformulation is also possible for systems oscillating at more than one frequency.⁴⁶

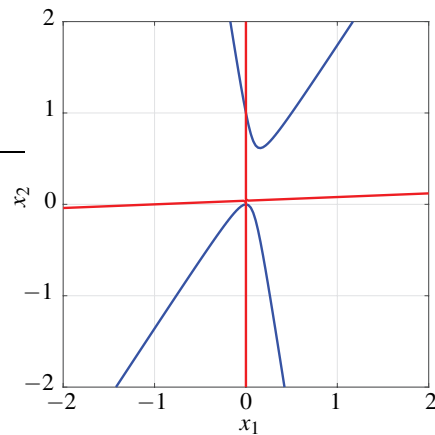


Figure 6. Singularity curves of the solutions \mathcal{N}_{12} and \mathcal{N}_{21} of Eqs. (28) (red) and (29) (blue), respectively, for the system of Shi Songling.^{54,75} Three of the four limit cycles of this system (not shown here, see Fig. 2 of Galias and Tucker⁵⁵) are tiny and encircle the point $(0,0)$. The fourth limit cycle encircles the point $(0,1)$. For a given system, similar curves as shown in this figure could be used as one-dimensional manifolds to seed initial conditions from for brute-force detection of limit cycles. In such an algorithm, the distances between intersections and critical points of the curves could serve as natural length scales for determining the discretization fineness in different regions.

In Sec. III B, a criterion was presented for ruling out closed orbits in certain regions of phase space of steady systems. From this general result, a corollary was derived which can be applied in automated fashion, yielding ordinary differential equations which can be easily solved. In contrast, applying Dulac’s criterion in automated fashion would yield (partial) differential inequalities, which are more complicated. As explained in Sec. IV H, these results could be used in the future for efficient and automated seeding of initial conditions in numerical algorithms to detect periodic solutions.^{47,84}

AUTHOR CONTRIBUTIONS

Tiemo Pedergnana: Conceptualization (lead), formal analysis, writing—original draft, writing—review and editing (lead). **Nicolas Noiray:** Conceptualization (supporting), supervision, writing—review and editing (supporting).

ACKNOWLEDGEMENTS

This project is funded by the Swiss National Science Foundation under Grant agreement 184617.

AUTHOR DECLARATIONS

Conflict of Interest

The authors have no conflicts to disclose.

DATA AVAILABILITY

The datasets used for generating the plots in this study can be directly obtained by numerical simulation of the related mathematical equations in the manuscript.

Appendix A: Reformulation of Bendixson's criterion

Bendixson's criterion concerns the steady planar system $\dot{x} = u(x)$. The criterion states that, if the divergence of u has a constant sign throughout a simply connected domain \mathcal{D} , then the system has no closed orbits fully contained in that domain. The coordinate-independent divergence operator for a vector field u in curvilinear coordinates is given by⁵³ (p. 92)

$$\operatorname{div} u(x) = \frac{1}{\sqrt{\det g(x)}} \nabla \cdot [\sqrt{\det g(x)} u(x)]. \quad (\text{A1})$$

Applying this operator to the RHS of Eq. (9) and requiring that the result be greater than zero yields

$$-\frac{1}{\sqrt{\det g(x)}} \nabla \cdot [\sqrt{\det g(x)} g^{-1}(x) \nabla \tilde{\mathcal{V}}(x)] > 0. \quad (\text{A2})$$

This requirement is simply the definition of a strictly subharmonic function⁵³ (p. 433), and the operator acting on $\tilde{\mathcal{V}}$ is the (negative) Laplace–Beltrami operator,⁵³ (p. 92) which arises here naturally from elementary manipulations. The analogous result for $-\tilde{\mathcal{V}}$ is obtained by replacing “>” with “<” in the inequality (A2).

Appendix B: Transformation formula for the Harmonic oscillator

In this appendix, we consider the noise-driven, forced-damped harmonic oscillator with position x_1 and normalized velocity $x_2 = \dot{x}_1/\omega_0$, whose dynamics are defined by the system

$$\dot{x} = \begin{pmatrix} \omega_0 x_2 \\ -\gamma x_2 - \omega_0 x_1 + \frac{F}{\omega_0} \cos \omega t + \frac{\xi}{\omega_0} \end{pmatrix}, \quad (\text{B1})$$

where ω_0 is the eigenfrequency, γ is the damping, F is the forcing amplitude and ξ is a zero-mean Gaussian white noise source with variance Γ . The HD of the planar system defined by Eq. (B1) can be written as follows:

$$\begin{aligned} \dot{x} = & \underbrace{-\left(\frac{\partial}{\partial x_1}\right) \left(\frac{\gamma x_2^2}{2} - \frac{F}{\omega_0} x_2 \cos \omega t\right)}_{=-\nabla \tilde{\mathcal{V}}(x,t)} + \underbrace{\left(\frac{\partial}{\partial x_2}\right) \frac{\omega_0 (x_1^2 + x_2^2)}{2}}_{=S \nabla \tilde{\mathcal{H}}(x)} \\ & + \underbrace{\begin{pmatrix} 0 \\ \xi \\ \omega_0 \end{pmatrix}}_{=\tilde{\Xi}}. \end{aligned} \quad (\text{B2})$$

Note that the HD in Eq. (B2) is only quasi-unique, as the forcing term could be neglected in the potential $\tilde{\mathcal{V}}$ and, instead, a term proportional to x_1 (specifically, $-[F x_1/\omega_0] \cos \omega t$) could be added to the Hamiltonian $\tilde{\mathcal{H}}$, leaving Eq. (B1) unchanged.

Next, we apply a transformation to amplitude-phase coordinates $y = (A, \phi)$, $A \in \mathbb{R}^+$, $\phi \in [0, 2\pi]$:

$$\underbrace{\begin{pmatrix} x_1 \\ x_2 \end{pmatrix}}_x = \underbrace{\begin{pmatrix} A \cos \phi \\ A \sin \phi \end{pmatrix}}_{f(y)}. \quad (\text{B3})$$

After substituting the expression (B3) into Eq. (B1), some algebraic manipulation and redefining $y \rightarrow x$, we find that the transformed dynamics are given by, with $x = (A, \phi)$:

$$\dot{x} = \begin{pmatrix} -\gamma A \sin^2 \phi + \frac{F}{\omega_0} \cos \omega t \sin \phi + \frac{\xi}{\omega_0} \sin \phi \\ -\omega_0 - \gamma \sin \phi \cos \phi + \frac{F}{\omega_0 A} \cos \omega t \cos \phi + \frac{\xi}{\omega_0 A} \cos \phi \end{pmatrix} \quad (\text{B4})$$

To confirm the transformation formula in Eq. (6), we compute the Jacobian matrix of the mapping (B3) and its polar decomposition:

$$J(x) = \underbrace{\begin{pmatrix} \cos \phi & -\sin \phi \\ \sin \phi & \cos \phi \end{pmatrix}}_{=Q(x)} \underbrace{\begin{pmatrix} 1 & 0 \\ 0 & A \end{pmatrix}}_{=h(x)}. \quad (\text{B5})$$

We observe that $\det Q = 1$. From the expressions in Eq. (B5), we immediately obtain the metric tensor $g = h^T h$ and its determinant:

$$g(x) = \operatorname{diag}(1, A^2), \quad (\text{B6})$$

$$\det g(x) = A^2. \quad (\text{B7})$$

Furthermore, we have $\tilde{\Xi} = Q^T \Xi = (\xi \sin \phi / \omega_0, \xi \cos \phi / \omega_0)^T$. By substituting the above expressions into Eq. (6), using the definitions $\tilde{\mathcal{V}}(x, t) = \mathcal{V}(f(x), t)$ and $\tilde{\mathcal{H}}(x, t) = \mathcal{H}(f(x), t)$, one can verify that the transformed dynamics, defined by Eq. (B4), are equivalent to

$$\begin{aligned} \dot{x} = & \underbrace{-\begin{pmatrix} 1 & 0 \\ 0 & A^{-2} \end{pmatrix}}_{=g^{-1}(x)} \underbrace{\left(\frac{\partial}{\partial A}\right) \left(\frac{\gamma A^2 \sin^2 \phi}{2} - \frac{F A}{\omega_0} \cos \omega t \sin \phi\right)}_{=\nabla \tilde{\mathcal{V}}(x,t)} \\ & + \underbrace{\frac{1}{A}}_{=\sqrt{\det g(x)}^{-1}} \underbrace{\left(\frac{\partial}{\partial \phi}\right) \left(\frac{\omega_0 A^2}{2}\right)}_{=S \nabla \tilde{\mathcal{H}}(x)} + \underbrace{\begin{pmatrix} 1 & 0 \\ 0 & A^{-1} \end{pmatrix}}_{=h^{-1}(x)} \underbrace{\begin{pmatrix} \tilde{\xi}_1 \\ \tilde{\xi}_2 \end{pmatrix}}_{=\tilde{\Xi}} \end{aligned} \quad (\text{B8})$$

confirming Eq. (6).

Appendix C: Polynomial Liénard systems

In first-order form, Liénard's equation reads as follows:⁶ (p. 212)

$$\dot{x} = \begin{pmatrix} x_2 \\ -p(x_1) - q(x_1)x_2 \end{pmatrix}. \quad (\text{C1})$$

We focus here on the class of nonlinear oscillators for which the antiderivative of p exists and q is given by a polynomial of finite order M :

$$q(x_1) = \sum_{m=1}^M q_m x_1^m. \quad (\text{C2})$$

The subclass for which $M \leq 2$ encompasses many well-known examples of linear and nonlinear oscillators, some of which are analyzed in this work. The bifurcations of a system of the form of Eq. (C1) with $M = 2$ for which p is a polynomial of order 5 have recently been analyzed.⁴⁶ A Liénard system, specified by Eq. (C1) with $M = 4$, has previously been studied in the context of thermoacoustic instabilities in turbulent combustors.⁷¹

Assuming a Cartesian basis, the Helmholtz decomposition (4) of the Liénard system governed by Eq. (C1) is given by

$$\begin{aligned} \mathcal{V}(x) &= \frac{q(x_1)x_2^2}{2} - q''(x_1)\frac{x_2^4}{24} + \dots \\ &= \sum_{n=0} q^{(2n)}(x_1) \frac{(-1)^n x_2^{2(n+1)}}{2(n+1)!}, \end{aligned} \quad (\text{C3})$$

$$\begin{aligned} \mathcal{H}(x) &= \frac{x_2^2}{2} + \int p(x_1) dx_1 + q'(x_1)\frac{x_2^3}{6} - q'''(x_1)\frac{x_2^5}{120} + \dots \\ &= \frac{x_2^2}{2} + \int p(x_1) dx_1 + \sum_{n=0} q^{(2n+1)}(x_1) \frac{(-1)^n x_2^{2n+3}}{(2n+3)!}, \end{aligned} \quad (\text{C4})$$

where a dash denotes the derivative, $\int p dx_1$ is the antiderivative of p and $q^{(n)}$ denotes the n^{th} derivative of q . This result can be verified by substituting the above expressions into Eq. (2), whereby the Eq. (C1) is recovered. The sums in Eqs. (C3) and (C4) truncate due to the finite order of q defined in Eq. (C2).

REFERENCES

- ¹R. Stratonovich, *Topics in the Theory of Random Noise Vol. I: General Theory of Random Processes Nonlinear Transformations of Signals and Noise* (Gordon & Breach, 1963).
- ²C. W. Gardiner et al., *Handbook of stochastic methods*, Vol. 4 (Springer Berlin, 1985).
- ³H. Risken, *The Fokker-Planck Equation* (Springer, 1984).
- ⁴Throughout this work, a dot over a dependent variable denotes the total time derivative.
- ⁵J. Guckenheimer and P. Holmes, *Nonlinear oscillations, dynamical systems, and bifurcations of vector fields*, Vol. 42 (Springer Science & Business Media, 2013).
- ⁶S. H. Strogatz, *Nonlinear dynamics and chaos: with applications to physics, biology, chemistry, and engineering* (CRC press, 2015).
- ⁷G. G. Stokes, "On the dynamical theory of diffraction," in *Mathematical and Physical Papers*, Cambridge Library Collection - Mathematics, Vol. 2 (Cambridge University Press, 2009) p. 243–328.
- ⁸H. Helmholtz, "Über Integrale der Hydrodynamischen Gleichungen, welche den Wirbelbewegungen entsprechen," *J. Reine Angew. Math.* **1858**, 25–55 (1858).
- ⁹P. M. Morse and H. Feshbach, *Methods of Theoretical Physics. Vol. 1-2* (New York, 1953).
- ¹⁰V. I. Arnold, *Mathematical methods of classical mechanics*, Vol. 60 (Springer Science & Business Media, 2013).
- ¹¹L. Morino, "Helmholtz decomposition revisited: Vorticity generation and trailing edge condition - part I: Incompressible flows," *Comput. Mech.* **1**, 65–90 (1986).
- ¹²D. Joseph, "Helmholtz decomposition coupling rotational to irrotational flow of a viscous fluid," *Proc. Natl. Acad. Sci. U.S.A.* **103**, 14272–14277 (2006).
- ¹³A. Linke, "On the role of the Helmholtz decomposition in mixed methods for incompressible flows and a new variational crime," *Comput. Methods Appl. Mech. Eng.* **268**, 782–800 (2014).
- ¹⁴O. Bühler, J. Callies, and R. Ferrari, "Wave-vortex decomposition of one-dimensional ship-track data," *J. Fluid Mech.* **756**, 1007–1026 (2014).
- ¹⁵E. Lindborg, "A Helmholtz decomposition of structure functions and spectra calculated from aircraft data," *J. Fluid Mech.* **762** (2014), 10.1017/jfm.2014.685.
- ¹⁶O. Bühler, M. Kuang, and E. Tabak, "Anisotropic Helmholtz and wave-vortex decomposition of one-dimensional spectra," *J. Fluid Mech.* **815**, 361–387 (2017).
- ¹⁷S. Schoder, K. Roppert, and M. Kaltenbacher, "Postprocessing of direct aeroacoustic simulations using Helmholtz decomposition," *AIAA J.* **58**, 3019–3027 (2020).
- ¹⁸J.-P. Caltagirone, "On a reformulation of Navier–Stokes equations based on Helmholtz–Hodge decomposition," *Phys. Fluids* **33** (2021), 10.1063/5.0053412.
- ¹⁹Y. Aharonov and D. Bohm, "Significance of electromagnetic potentials in the quantum theory," *Phys. Rev.* **115**, 485–491 (1959).
- ²⁰E. Konopinski, "What the electromagnetic vector potential describes," *Am. J. Phys.* **46**, 499–502 (1978).
- ²¹E. Haber, U. Ascher, D. Aruliah, and D. Oldenburg, "Fast simulation of 3d electromagnetic problems using potentials," *J. Comput. Phys.* **163**, 150–171 (2000).
- ²²F. W. Hehl and Y. N. Obukhov, *Foundations of classical electrodynamics: Charge, flux, and metric*, Vol. 33 (Springer Science & Business Media, 2003).
- ²³C. Weiss, "Project APhiD: A Lorenz-gauged $A - \phi$ decomposition for parallelized computation of ultra-broadband electromagnetic induction in a fully heterogeneous earth," *Comput. Geosci.* **58**, 40–52 (2013).
- ²⁴Q. Du, C. Guo, Q. Zhao, X. Gong, C. Wang, and X.-Y. Li, "Vector-based elastic reverse time migration based on scalar imaging condition," *Geophysics* **82**, S111–S127 (2017).
- ²⁵Y. Shi, W. Zhang, and Y. Wang, "Seismic elastic RTM with vector-wavefield decomposition," *J. Geophys. Eng.* **16**, 509–524 (2019).
- ²⁶D. Paganin and K. Nugent, "Noninterferometric phase imaging with partially coherent light," *Phys. Rev. Lett.* **80**, 2586–2589 (1998).
- ²⁷E. Park and A. Maniatty, "Shear modulus reconstruction in dynamic elastography: Time harmonic case," *Phys. Med. Biol.* **51**, 3697–3721 (2006).
- ²⁸T. Kohlberger, E. Mémin, and C. Schnörr, "Variational dense motion estimation using the Helmholtz decomposition," *Lect. Notes Comput. Sci.* **2695**, 432–448 (2003).
- ²⁹Q. Guo, M. Mandal, and M. Li, "Efficient Hodge-Helmholtz decomposition of motion fields," *Pattern Recognit. Lett.* **26**, 493–501 (2005).
- ³⁰A. Cuzol, P. Hellier, and E. Mémin, "A low dimensional fluid motion estimator," *Int. J. Comput. Vis.* **75**, 329–349 (2007).
- ³¹C. G. Simader and H. Sohr, "A new approach to the Helmholtz decomposition and the Neumann problem in L^q -spaces for bounded and exterior domains," in *Mathematical Problems Relating to the Navier-Stokes Equations*, Series on Advances in Mathematics for Applied Sciences, Vol. 11 (World Scientific Publishing, 1992) pp. 1–35.
- ³²R. Farwig, H. Kozono, and H. Sohr, "On the Helmholtz decomposition in general unbounded domains," *Arch. Math.* **88**, 239–248 (2007).

- ³³H. Sohr, *The Navier–Stokes equations: An elementary functional analytic approach* (Springer Science & Business Media, 2012).
- ³⁴H. E. Moses, “Eigenfunctions of the curl operator, rotationally invariant helmholtz theorem, and applications to electromagnetic theory and fluid mechanics,” *SIAM J. Appl. Math.* **21**, 114–144 (1971).
- ³⁵B. Schweizer, “On Friedrichs inequality, Helmholtz decomposition, vector potentials, and the div-curl lemma,” in *Trends in Applications of Mathematics to Mechanics*, edited by E. Rocca, U. Stefanelli, L. Truskinovsky, and A. Visintin (Springer International Publishing, Cham, 2018) pp. 65–79.
- ³⁶Y. Giga and Z. Gu, “The Helmholtz decomposition of a space of vector fields with bounded mean oscillation in a bounded domain,” *Math. Ann.* (2022), 10.1007/s00208-022-02410-y.
- ³⁷E. Glötzl and O. Richters, “Helmholtz decomposition and potential functions for n-dimensional analytic vector fields,” *J. Math. Anal. Appl.* **525** (2023), 10.1016/j.jmaa.2023.127138.
- ³⁸H. Bhatia, G. Norgard, V. Pascucci, and P.-T. Bremer, “The Helmholtz-hodge decomposition - a survey,” *IEEE Trans. Vis. Comput. Graph.* **19**, 1386–1404 (2013).
- ³⁹R. A. Horn and C. R. Johnson, *Matrix analysis* (Cambridge University press, 2012).
- ⁴⁰Note that, by the uniqueness of the Cholesky decomposition for positive definite matrices,³⁹ (see p. 441) the polar decomposition $J = Qh$ and the QR factorization³⁹ (see p. 449) of J coincide, which implies that h^{-1} is generally a lower triangular matrix.
- ⁴¹T. Pedergnana and N. Noiray, “Exact potentials in multivariate Langevin equations,” *Chaos* **32** (2022), 10.1063/5.0124031.
- ⁴²V. Guillemin and A. Pollack, *Differential topology*, Vol. 370 (American Mathematical Society, 2010).
- ⁴³F. González-Gascón, “Note on paper of Andrey concerning non-Hamiltonian systems,” *Phys. Lett. A* **114**, 61 – 62 (1986).
- ⁴⁴Y. Nutku, “Hamiltonian structure of the Lotka-Volterra equations,” *Phys. Lett. A* **145**, 27 – 28 (1990).
- ⁴⁵An “orbit” is a curve in the (frozen) phase space of a steady dynamical system along which a trajectory runs.
- ⁴⁶J. del Pino, J. Kořata, and O. Zilberberg, “Limit cycles as stationary states of an extended harmonic balance ansatz,” (2023), arXiv:2308.06092 [nlin.AO].
- ⁴⁷T. S. Parker and L. Chua, *Practical numerical algorithms for chaotic systems* (Springer Science & Business Media, 2012).
- ⁴⁸M. Han, “Bifurcation theory of limit cycles of planar systems,” in *Handbook of Differential Equations: Ordinary Differential Equations*, Vol. 3 (Elsevier, 2006) pp. 341–433.
- ⁴⁹D. Hilbert, “Mathematische Probleme,” *Nachrichten von der Königlichen Gesellschaft der Wissenschaften zu Göttingen* (1900).
- ⁵⁰Y. Ilyashenko, “Centennial history of hilbert’s 16th problem,” *Bull. Am. Math. Soc.* **39**, 301 – 354 (2002).
- ⁵¹S. Busenberg and P. D. Van Den, “A method for proving the non-existence of limit cycles,” *J. Math. Anal. Appl.* **172**, 463 – 479 (1993).
- ⁵²The limiting case of a closed orbit which is a fixed point is excluded from the discussion here.
- ⁵³J. Jost, *Riemannian geometry and geometric analysis*, Vol. 42005 (Springer, 2011).
- ⁵⁴S. Shi, “Concrete example of the existence of 4 limit-cycles for plane quadratic systems,” *Sci. Sin.* **23**, 153–158 (1980).
- ⁵⁵Z. Galias and W. Tucker, “The Songling system has exactly four limit cycles,” *Appl. Math. Comput.* **415** (2022), 10.1016/j.amc.2021.126691.
- ⁵⁶S. Särkkä and A. Solin, *Applied stochastic differential equations*, Vol. 10 (Cambridge University Press, 2019).
- ⁵⁷R. Abraham, J. E. Marsden, and T. Ratiu, *Manifolds, tensor analysis, and applications*, Vol. 75 (Springer Science & Business Media, 2012).
- ⁵⁸P. J. Olver, *Applications of Lie groups to differential equations*, Vol. 107 (Springer Science & Business Media, 1993).
- ⁵⁹G. Quispel and H. Capel, “Solving odes numerically while preserving a first integral,” *Phys. Lett. A* **218**, 223 – 228 (1996).
- ⁶⁰R. I. McLachlan, G. Quispel, and N. Robidoux, “Unified approach to Hamiltonian systems, Poisson systems, gradient systems, and systems with Lyapunov functions or first integrals,” *Phys. Rev. Lett.* **81**, 2399 – 2403 (1998).
- ⁶¹R. I. McLachlan, G. Quispel, and N. Robidoux, “Geometric integration using discrete gradients,” *Philos. Trans. R. Soc. A* **357**, 1021 – 1045 (1999).
- ⁶²T. Bárta, R. Chill, and E. Fašangová, “Every ordinary differential equation with a strict Lyapunov function is a gradient system,” *Monatsh. Math.* **166**, 57 – 72 (2012).
- ⁶³Unless u vanishes identically, in which case there is nothing to prove.
- ⁶⁴W. Kermack and A. McKendrick, “Contributions to the mathematical theory of epidemics-I,” *Bull. Math. Biol.* **53**, 33 – 55 (1991).
- ⁶⁵Y. Nutku, “Bi-Hamiltonian structure of the Kermack-McKendrick model for epidemics,” *Journal of Physics A: Mathematical and General* **23**, L1145–L1146 (1990).
- ⁶⁶A. Ballesteros, A. Blasco, and I. Gutierrez-Sagredo, “Hamiltonian structure of compartmental epidemiological models,” *Phys. D: Nonlinear Phenom.* **413** (2020), 10.1016/j.physd.2020.132656.
- ⁶⁷K. O’Keeffe, S. Ceron, and K. Petersen, “Collective behavior of swarmalators on a ring,” *Phys. Rev. E* **105** (2022).
- ⁶⁸T. Pedergnana and N. Noiray, “Superradiant scattering by a limit cycle,” *Phys. Rev. Applied* **20**, 034068 (2023).
- ⁶⁹J. A. Sanders, F. Verhulst, and J. Murdock, *Averaging methods in nonlinear dynamical systems*, Vol. 59 (Springer, Berlin, Heidelberg, 2007).
- ⁷⁰J. Roberts and P. Spanos, “Stochastic averaging: An approximate method of solving random vibration problems,” *Int. J. Non-Linear Mech.* **21**, 111–134 (1986).
- ⁷¹N. Noiray, “Linear growth rate estimation from dynamics and statistics of acoustic signal envelope in turbulent combustors,” *J. Eng. Gas Turbines Power* **139** (2017), 10.1115/1.4034601.
- ⁷²A. Balanov, N. Janson, D. Postnov, and O. Sosnovtseva, *From simple to complex* (Springer, Berlin, Heidelberg, 2009).
- ⁷³B. Van der Pol, “LXXXVIII. on “relaxation-oscillations,”” *London Edinburgh Philos. Mag. J. Sci.* **2**, 978–992 (1926).
- ⁷⁴G. Duffing, *Erzwungene Schwingungen bei veränderlicher Eigenfrequenz und ihre technische Bedeutung*, 41–42 (Vieweg, 1918) pp. 1–134.
- ⁷⁵S. Songling, “A method of constructing cycles without contact around a weak focus,” *J. Differ. Equ.* **41**, 301 – 312 (1981).
- ⁷⁶N. Kuznetsov, O. Kuznetsova, and G. Leonov, “Visualization of four normal size limit cycles in two-dimensional polynomial quadratic system,” *Differ. Equ. Dyn. Syst.* **21**, 29 – 34 (2013).
- ⁷⁷P. A. M. Dirac, *The principles of quantum mechanics*, 27 (Oxford university press, 1981).
- ⁷⁸N. Moiseyev, *Non-Hermitian quantum mechanics* (Cambridge University Press, 2011).
- ⁷⁹S. Deguchi and Y. Fujiwara, “Quantization of the damped harmonic oscillator based on a modified Bateman Lagrangian,” *Phys. Rev. A* **101** (2020), 10.1103/PhysRevA.101.022105.
- ⁸⁰M. J. Blacker and D. L. Tilbrook, “Alternative approach to the quantization of the damped harmonic oscillator,” *Phys. Rev. A* **104** (2021), 10.1103/PhysRevA.104.032211.
- ⁸¹A. Eichler and O. Zilberberg, *Classical and Quantum Parametric Phenomena* (Oxford University Press, 2023).
- ⁸²O. Esen, M. Grmela, and M. Pavelka, “On the role of geometry in statistical mechanics and thermodynamics. I. Geometric perspective,” *J. Math. Phys.* **63** (2022), 10.1063/5.0099923.
- ⁸³H. Waalkens, R. Schubert, and S. Wiggins, “Wigner’s dynamical transition state theory in phase space: Classical and quantum,” *Nonlinearity* **21**, R1–R118 (2008).
- ⁸⁴M. Jahn, M. Stender, S. Tatzko, N. Hoffmann, A. Grollet, and J. Wallaschek, “The extended periodic motion concept for fast limit cycle detection of self-excited systems,” *Comput. Struct.* **227** (2020), 10.1016/j.compstruc.2019.106139.